INTERNATIONAL JOURNAL FOR NUMERICAL METHODS IN ENGINEERING, VOL. 24, 893–911 (1987)

SUBSTEPPING SCHEMES FOR THE NUMERICAL INTEGRATION OF ELASTOPLASTIC STRESS–STRAIN RELATIONS

S. W. SLOAN

Department of Civil Engineering and Surveying, University of Newcastle, N.S.W. 2308, Australia

SUMMARY

This paper describes two substepping schemes for integrating elastoplastic stress–strain relations. The schemes are designed for use in finite element plasticity calculations and solve for the stress increments assuming that the strain increments are known. Both methods are applicable to a general type of constitutive law and control the error in the integration process by adjusting the size of each substep automatically. The first method is based on the well-known modified Euler scheme, whereas the second technique employs a high order Runge–Kutta formula. The procedures outlined do not require any form of stress correction to prevent drift from the yield surface. Their utility is illustrated by analysis of typical boundary value problems.

INTRODUCTION

When the displacement type of finite element method is used to analyse the behaviour of elastoplastic solids, the overall load–deformation response is ascertained in an incremental or iterative manner. At each stage in the solution process the external forces are applied in increments and the corresponding nodal displacement increments are determined via the global stiffness equations. The strains and stresses are then computed at a discrete number of integration points within each element using the strain–displacement relations and the elastoplastic stress–strain law, respectively. If the stresses at an integration point cause plastic yielding and an isotropic hardening rule is employed, the stresses are found by solving a system of differential equations of the form

$$\dot{\boldsymbol{\sigma}} = \mathbf{D}_{\mathrm{ep}}(\boldsymbol{\sigma}, \kappa)\left(\frac{\Delta \boldsymbol{\varepsilon}}{\Delta t}\right) = \mathbf{D}_{\mathrm{ep}}(\boldsymbol{\sigma}, \kappa)\dot{\boldsymbol{\varepsilon}} \tag{1}$$

where $\boldsymbol{\sigma}$ denotes a vector of stresses, $\boldsymbol{\varepsilon}$ denotes a vector of strains, κ is some hardening parameter, $\mathbf{D}_{\mathrm{ep}}$ denotes the elastoplastic stress–strain matrix, the superior dot represents a derivative with respect to time and Δt is the time interval over which the external forces have been applied. Since the stresses and hardening parameter are known at the beginning of the time interval, and the known strain rates may be assumed to be constant throughout the time interval, equation (1) defines an initial value problem.

In finite element codes, the first-order Euler scheme is often used to solve for the unknown stresses in equation (1). As the Euler scheme is accurate only for very small time steps, it is usual to subdivide Δt into smaller substeps and compute the stress–strain response over each substep.[1,2] Traditionally, the number of substeps is determined from an empirical rule and each substep is assumed to be of the same size. A disadvantage of this approach is that the computed stresses may not satisfy the yield criterion at the end of each time interval, and it is necessary to apply some form

0029–5981/87/050893–19$09.50

Received 10 February 1985
Revised 2 September 1986

of correction to restore them to the yield surface. In general it is difficult to establish a theoretical basis for this procedure and, although the corrected stresses may satisfy the yield condition approximately, the plastic deformations may not obey the prescribed flow rule.

This paper describes two general schemes for integrating elastoplastic stress–strain laws to obtain the unknown stresses. Both methods assume known strain increments and solve for the corresponding elastoplastic stress increments. A key feature of the proposed schemes is that they attempt to control the error in the integration process by selecting the size of each substep automatically as the integration proceeds over each time interval. The first method is based on the well-known modified Euler scheme, whereas the second procedure uses the Runge–Kutta formulae developed by England.[3] Neither of the algorithms requires any form of stress correction and they are both adaptations of methods that are used widely in the numerical analysis literature. The ability of the schemes to control the error in the integration of elastoplastic constitutive laws, for a given spatial discretization and loading programme, is illustrated by analysis of a typical boundary value problem. Results are presented for two smooth rigid strip footings: one resting on a perfectly plastic Mohr–Coulomb layer and the other resting on a strain-hardening Tresca layer.

ELASTOPLASTIC STRESS–STRAIN RELATIONS

In the classical theory of plasticity, the total strain rate is decomposed into elastic and plastic components according to the equation

$$\dot{\boldsymbol{\varepsilon}} = \dot{\boldsymbol{\varepsilon}}_e + \dot{\boldsymbol{\varepsilon}}_p \tag{2}$$

where plastic straining occurs only after the yield condition is reached and the elastic strain rates are given by Hooke's law

$$\dot{\boldsymbol{\varepsilon}}_e = \mathbf{D}^{-1}\dot{\boldsymbol{\sigma}} \tag{3}$$

In the current work the yield function, which defines the limit of elastic behaviour, is defined to be of the form

$$F(\boldsymbol{\sigma}, \kappa) = 0 \tag{4}$$

where $\boldsymbol{\sigma}$ denotes the current stresses and κ is some hardening parameter which depends on the history of deformation. At the onset of plastic yielding, the plastic strain rates are assumed to be governed by a flow rule of the form

$$\dot{\boldsymbol{\varepsilon}}_p = \dot{\lambda}\frac{\partial Q}{\partial \boldsymbol{\sigma}} = \dot{\lambda}\mathbf{b} \tag{5}$$

where $\dot{\lambda}$ is a positive multiplier, $\mathbf{b} = \partial Q/\partial \boldsymbol{\sigma}$ and Q is the plastic potential. The plastic potential is defined in a similar fashion to the yield function and is given by

$$Q(\boldsymbol{\sigma}, \kappa) = 0 \tag{6}$$

If the yield function is assumed to be coincident with the plastic potential, the flow rule is said to be associated and the matrix $\mathbf{D}_{ep}$ is symmetric. If this is not the case, the flow rule is said to be non-associated and the matrix $\mathbf{D}_{ep}$ is in general non-symmetric.

Using equations (2)–(6), together with the assumption that $\mathrm{d}F = 0$ during plastic yielding, leads to the well-known elastoplastic stress–strain relations, which may be expressed as

$$\dot{\boldsymbol{\sigma}} = (\mathbf{D} - \mathbf{D}_p)\dot{\boldsymbol{\varepsilon}} = \mathbf{D}_{ep}\dot{\boldsymbol{\varepsilon}} \tag{7}$$

where the matrix $\mathbf{D}_p$ is given by

$$\mathbf{D}_p = \frac{\mathbf{D}\mathbf{b}\mathbf{a}^T\mathbf{D}}{A + \mathbf{a}^T\mathbf{D}\mathbf{b}} \tag{8}$$

and

$$\mathbf{a} = \frac{\partial F}{\partial \boldsymbol{\sigma}} \tag{9}$$

$$A = -\frac{1}{\dot{\lambda}}\frac{\partial F}{\partial \kappa}\dot{\kappa} \tag{10}$$

The explicit form of the hardening modulus, defined by equation (10), depends on the type of hardening model that is adopted. For an isotropic strain-hardening model, which will be employed later in this paper, the hardening parameter is assumed to be related to some measure of the plastic strains via the equation

$$\dot{\kappa} = \dot{\bar{\varepsilon}}_p \tag{11}$$

where

$$\dot{\bar{\varepsilon}}_p = \dot{\lambda}\{\bar{\mathbf{b}}^T\bar{\mathbf{b}}\}^{1/2} = \dot{\lambda}\|\bar{\mathbf{b}}\| \tag{12}$$

and

$$\bar{\mathbf{b}}^T = \left\{\sqrt{2}\frac{\partial Q}{\partial \sigma_x}, \sqrt{2}\frac{\partial Q}{\partial \sigma_y}, \sqrt{2}\frac{\partial Q}{\partial \sigma_z}, \frac{\partial Q}{\partial \tau_{xy}}, \frac{\partial Q}{\partial \tau_{yz}}, \frac{\partial Q}{\partial \tau_{zx}}\right\} \tag{13}$$

In other hardening models, such as the isotropic work hardening law discussed by Hill,[4] the hardening parameter may be assumed to be related to the plastic work according to

$$\dot{\kappa} = \dot{W}_p \tag{14}$$

where

$$\dot{W}_p = \boldsymbol{\sigma}^T\dot{\boldsymbol{\varepsilon}}_p = \dot{\lambda}\boldsymbol{\sigma}^T\mathbf{b} \tag{15}$$

Both of the above models require integration over the strain path to give the appropriate value of the hardening parameter and, hence, the hardening modulus.

Finally, for numerical computation, we note that it is convenient to rewrite equation (7) as

$$\dot{\boldsymbol{\sigma}} = \dot{\boldsymbol{\sigma}}_e - \dot{\lambda}\mathbf{D}\mathbf{b} \tag{16}$$

where

$$\dot{\lambda} = \frac{\mathbf{a}^T\dot{\boldsymbol{\sigma}}_e}{A + \mathbf{a}^T\mathbf{D}\mathbf{b}} \tag{17}$$

and

$$\dot{\boldsymbol{\sigma}}_e = \mathbf{D}\dot{\boldsymbol{\varepsilon}} \tag{18}$$

denotes the elastic stress rate. Expressing the stress–strain relations in this form allows for the possibility of plastic unloading. If $\dot{\lambda}$ is found to be less than zero during a time step, then $\dot{\lambda}$ is set to zero and the correct stress rate is simply given by $\dot{\boldsymbol{\sigma}} = \dot{\boldsymbol{\sigma}}_e$.

DETERMINATION OF INITIAL YIELDING

For analysis of the load–deformation behaviour of elastoplastic materials with the displacement finite element method, it is necessary to apply the external forces incrementally. Following the application of a load step, the strain increments at an integration point may be computed from the

strain–displacement relations according to

$$\Delta \mathbf{e} = \mathbf{B}\Delta \mathbf{u} \tag{19}$$

where $\mathbf{B}$ denotes the strain–displacement matrix and $\Delta \mathbf{u}$ is the vector of nodal displacement increments for the current load step (or iteration). Once the strains have been determined, the elastic stress increments may be calculated using Hooke's law:

$$\Delta \boldsymbol{\sigma} = \mathbf{D}\Delta \mathbf{e} \tag{20}$$

At any stage during the solution process the stress–strain behaviour at an integration point will either be 'elastic' or 'plastic'. If a point changes from an elastic to a plastic state, it is necessary to determine the portion of the stress increment that causes purely elastic deformation. Let $\boldsymbol{\sigma}_a$ denote the stresses at the beginning of a load step such that

$$F(\boldsymbol{\sigma}_a, \kappa) = F_a < 0$$

where the hardening parameter κ remains constant while deformation takes place within the yield surface. By definition, plastic yielding must occur if

$$F(\boldsymbol{\sigma}_a + \Delta\boldsymbol{\sigma}, \kappa) = F(\boldsymbol{\sigma}_b, \kappa) = F_b > 0$$

In order to determine the portion of the stress increment that lies within the yield surface, we need to find a scalar α such that

$$F(\boldsymbol{\sigma}, \kappa) = 0 \tag{21}$$

where

$$\boldsymbol{\sigma} = \boldsymbol{\sigma}_a + \alpha\Delta\boldsymbol{\sigma}, \quad 0 < \alpha < 1 \tag{22}$$

A first guess for α may be obtained by a simple linear interpolation in F which gives

$$\alpha_1 = \frac{F_a}{F_a - F_b} \tag{23}$$

Since equations (21) and (22) define a single non-linear equation of the form $F(\alpha) = 0$, more accurate estimates for α may be obtained by a variety of iterative schemes. Using the Newton–Raphson technique, for example, the stresses and α are updated using the relations

$$\begin{aligned} \boldsymbol{\sigma}_k &= \boldsymbol{\sigma}_{k-1} + \alpha_k \Delta\boldsymbol{\sigma} \\ \alpha_{k+1} &= \alpha_k - \frac{F(\boldsymbol{\sigma}_k, \kappa)}{\mathbf{a}_k^{\mathrm{T}} \Delta\boldsymbol{\sigma}} \end{aligned} \tag{24}$$

where the vector $\mathbf{a}_k = (\partial F/\partial \boldsymbol{\sigma})_k$ is evaluated at the stress $\boldsymbol{\sigma}_k$. This iterative procedure may be started by assuming $\boldsymbol{\sigma}_0 = \boldsymbol{\sigma}_a$ and using α_1 from equation (23). Equation (24) stems from the standard update for a Newton–Raphson iteration which is

$$\alpha_{k+1} = \alpha_k + \Delta\alpha_{k+1}$$

where

$$\Delta\alpha_{k+1} = \frac{-F(\boldsymbol{\sigma}_k, \kappa)}{\left(\dfrac{\partial F}{\partial \alpha}\right)} = \frac{-F(\boldsymbol{\sigma}_k, \kappa)}{\mathbf{a}_k^{\mathrm{T}} \dfrac{\partial \boldsymbol{\sigma}}{\partial \alpha}} = \frac{-F(\boldsymbol{\sigma}_k, \kappa)}{\mathbf{a}_k^{\mathrm{T}} \Delta\boldsymbol{\sigma}}$$

The iteration procedure for determining α and $\boldsymbol{\sigma}$ may be terminated when the relative error in the norm of the stresses, defined by $\|\boldsymbol{\sigma}_{k+1} - \boldsymbol{\sigma}_k\|/\|\boldsymbol{\sigma}_k\|$, is less than some specified tolerance.

For a secant iteration scheme, which does not require the evaluation of the gradient vector **a**, equation (24) is replaced by

$$\alpha_{k+1} = \alpha_k - \frac{F(\boldsymbol{\sigma}_k, \kappa)}{F(\boldsymbol{\sigma}_k, \kappa) - F(\boldsymbol{\sigma}_{k-1}, \kappa)}(\alpha_k - \alpha_{k-1})$$

where the starting values are $\boldsymbol{\sigma}_0 = \boldsymbol{\sigma}_a, \alpha_0 = 0$ and α_1 from equation (23).

Owing to the good initial guess that is available for α, both the Newton–Raphson and secant algorithms have been found to converge rapidly when implemented in finite element codes. Indeed, even with large load increments and a tight error tolerance on the stresses ($\approx 10^{-10}$), both algorithms typically converge within 4 or 5 iterations. Experience suggests that the α values obtained from linear interpolation, if used without further refinement, are not sufficiently accurate for many plasticity calculations. In general, some form of iteration is necessary if the plastic deformations are large or the yield criterion is highly non-linear. For double precision arithmetic on a 32-bit machine, tolerances for the relative error in the norm of the stresses are typically less than 10^{-6}.

EULER INTEGRATION SCHEME WITH STRESS CORRECTION

Once the stresses at the onset of initial yielding have been computed, the elastoplastic stresses for a general isotropic hardening model are determined by solving the pair of rate equations

$$\dot{\boldsymbol{\sigma}} = \mathbf{D}_{ep}(\boldsymbol{\sigma}, \kappa)\dot{\mathbf{e}} = \mathbf{D}_{ep}(\boldsymbol{\sigma}, \kappa)\left(\frac{\Delta \mathbf{e}}{\Delta t}\right) \tag{25}$$

$$\dot{\kappa} = \begin{cases} \dot{\bar{\varepsilon}}_p, & \text{strain hardening} \\ \dot{W}_p, & \text{work hardening} \end{cases} \tag{26}$$

over the interval $(1-\alpha)\Delta t$. Let t^i and t^{i+1} denote the time at the onset of plastic yielding and the time at the end of the load step (or iteration), respectively. Then $t^{i+1} = t^i + (1-\alpha)\Delta t$ and the interval over which plastic yielding occurs is $t^i \leqslant t \leqslant t^{i+1}$. If we define a 'dimensionless time', T, such that

$$T = \frac{t - t^i}{t^{i+1} - t^i} = \frac{t - t^i}{(1-\alpha)\Delta t}, \quad 0 \leqslant T \leqslant 1$$

then equations (25) and (26) may be written in a form which is convenient for numerical solution. Noting that

$$\dot{\boldsymbol{\sigma}} = \frac{1}{(1-\alpha)\Delta t}\frac{\mathrm{d}\boldsymbol{\sigma}}{\mathrm{d}T}$$

equation (25) may be expressed as

$$\frac{\mathrm{d}\boldsymbol{\sigma}}{\mathrm{d}T} = \mathbf{D}_{ep}(\boldsymbol{\sigma}, \kappa)\Delta\boldsymbol{\varepsilon} \tag{27}$$

where

$$\Delta\boldsymbol{\varepsilon} = (1-\alpha)\Delta\mathbf{e}$$

Using equations (11)–(15), together with equation (17), the differential equation for the hardening parameter becomes

$$\frac{\mathrm{d}\kappa}{\mathrm{d}T} = \begin{cases} \Delta\lambda(\boldsymbol{\sigma}, \kappa, \Delta\boldsymbol{\varepsilon})\|\bar{\mathbf{b}}\|, & \text{strain hardening} \\ \Delta\lambda(\boldsymbol{\sigma}, \kappa, \Delta\boldsymbol{\varepsilon})\boldsymbol{\sigma}^{\mathrm{T}}\mathbf{b}, & \text{work hardening} \end{cases} \tag{28}$$

where

$$\Delta\lambda(\boldsymbol{\sigma}, \kappa, \Delta\boldsymbol{\varepsilon}) = \left(\frac{\mathbf{a}^{\mathrm{T}}\mathbf{D}}{A + \mathbf{a}^{\mathrm{T}}\mathbf{D}\mathbf{b}}\right)\Delta\boldsymbol{\varepsilon}$$

Equations (27) and (28) now define a classical initial value problem, since $\Delta\boldsymbol{\varepsilon}$ is known and the right hand sides are functions of $\boldsymbol{\sigma}$ and κ. The interval of integration is $0 \leqslant T \leqslant 1$, where $T = 0$ corresponds to time t^i and $T = 1$ corresponds to time t^{i+1}. The initial conditions are the known stresses and hardening parameter at time t^i, which will be denoted $\boldsymbol{\sigma}^i$ and κ^i, respectively.

The crudest method for solving the system of differential equations defined by (27) and (28) is the Euler algorithm. This procedure gives the stresses and hardening parameter at time t^{i+1} according to

$$\boldsymbol{\sigma}^{i+1} = \boldsymbol{\sigma}^i + \mathbf{D}_{\mathrm{ep}}(\boldsymbol{\sigma}^i, \kappa^i)\Delta\boldsymbol{\varepsilon}$$

$$\kappa^{i+1} = \kappa^i + \begin{cases} \Delta\lambda(\boldsymbol{\sigma}^i, \kappa^i, \Delta\boldsymbol{\varepsilon})\|\bar{\mathbf{b}}\|^i, & \text{strain hardening} \\ \Delta\lambda(\boldsymbol{\sigma}^i, \kappa^i, \Delta\boldsymbol{\varepsilon})(\boldsymbol{\sigma}^i)^{\mathrm{T}}\mathbf{b}^i, & \text{work hardening} \end{cases}$$

where $\|\bar{\mathbf{b}}\|^i$ and $\mathbf{b}^i$ are evaluated at the stress $\boldsymbol{\sigma}^i$ and ΔT, the increment in the dimensionless time T, is assumed to be unity. Although the Euler method is accurate only for very small time steps, it is often used in finite element programs. As noted by Nayak and Zienkiewicz,[1] the accuracy of this procedure is improved if the time step $\Delta T = 1$ is broken up into a number of smaller time steps of equal size. Letting M denote the number of substeps, the size of each substep is given by $\Delta T_k = 1/M$ and the stresses and hardening parameter are updated using the formulae

$$\boldsymbol{\sigma}_{k+1} = \boldsymbol{\sigma}_k + \mathbf{D}_{\mathrm{ep}}(\boldsymbol{\sigma}_k, \kappa_k)\Delta\boldsymbol{\varepsilon}_k$$

$$\kappa_{k+1} = \kappa_k + \begin{cases} \Delta\lambda(\boldsymbol{\sigma}_k, \kappa_k, \Delta\boldsymbol{\varepsilon}_k)\|\bar{\mathbf{b}}\|_k, & \text{strain hardening} \\ \Delta\lambda(\boldsymbol{\sigma}_k, \kappa_k, \Delta\boldsymbol{\varepsilon}_k)\boldsymbol{\sigma}_k^{\mathrm{T}}\mathbf{b}_k, & \text{work hardening} \end{cases}$$

where $\Delta\boldsymbol{\varepsilon}_k = \Delta T_k \Delta\boldsymbol{\varepsilon}$ and $k = 1, 2, \ldots, M$. The process is started by setting $\boldsymbol{\sigma}_1 = \boldsymbol{\sigma}^i$ and $\kappa_1 = \kappa^i$, and the values of the stresses and the hardening parameter at the end of the interval are given by $\boldsymbol{\sigma}^{i+1} = \boldsymbol{\sigma}_{M+1}$ and $\kappa^{i+1} = \kappa_{M+1}$, respectively. When applying this algorithm the number of substeps required for each integration point is usually estimated empirically.[1,2] Since the errors in the stresses are not controlled directly, however, the stresses and hardening parameter at time t^{i+1} may not necessarily satisfy the yield criterion, i.e.

$$F(\boldsymbol{\sigma}^{i+1}, \kappa^{i+1}) \neq 0$$

As any deviations from the yield condition are cumulative and may result in unacceptable errors in subsequent computations, the stresses are often 'corrected' in an attempt to satisfy the current yield condition. Because there is no unique way to scale the stresses, it is usually assumed that the correction is applied along a direction which is normal to the yield function. Following this assumption we may write

$$\delta\boldsymbol{\sigma} = \beta\frac{\partial F}{\partial \boldsymbol{\sigma}} = \beta\mathbf{a}$$

where $\delta\boldsymbol{\sigma}$ is the stress correction vector and β is a scalar. In order to find the stresses that lie on the current yield surface (assuming that the current value of the hardening parameter is correct), we need to find the scalar β such that

$$F(\boldsymbol{\sigma}, \kappa^{i+1}) = 0 \tag{29}$$

where

$$\boldsymbol{\sigma} = \boldsymbol{\sigma}^{i+1} + \delta\boldsymbol{\sigma} = \boldsymbol{\sigma}^{i+1} + \beta \mathbf{a}^{i+1} \tag{30}$$

and the vector $\mathbf{a}^{i+1} = (\partial F/\partial \boldsymbol{\sigma})^{i+1}$ is evaluated at the stress $\boldsymbol{\sigma}^{i+1}$.

Equations (29) and (30) define a single non-linear equation of the form $F(\beta) = 0$ and may be solved iteratively. Adopting a Newton–Raphson strategy, for example, improved values for β and the stresses may be found using

$$\beta_k = \beta_{k-1} - \frac{F(\boldsymbol{\sigma}_{k-1}, \kappa^{i+1})}{\mathbf{a}_{k-1}^{\mathrm{T}} \mathbf{a}^{i+1}} \tag{31}$$

$$\boldsymbol{\sigma}_k = \boldsymbol{\sigma}_{k-1} + \beta_k \mathbf{a}^{i+1} \tag{32}$$

where $\mathbf{a}_{k-1} = (\partial F/\partial \boldsymbol{\sigma})_{k-1}$ is evaluated at the stress $\boldsymbol{\sigma}_{k-1}$ and the hardening parameter κ^{i+1} is constant. The procedure is started by setting $\boldsymbol{\sigma}_0 = \boldsymbol{\sigma}^{i+1}$ and $\beta_0 = 0$, and may be terminated as soon as $\|\boldsymbol{\sigma}_k - \boldsymbol{\sigma}_{k-1}\|/\|\boldsymbol{\sigma}_{k-1}\|$ is less than some specified tolerance.

Instead of iterating with equations (31) and (32) until convergence is achieved, it is often assumed that departures from the yield surface are small and that one iteration is sufficient. This gives

$$\beta_1 = \frac{-F(\boldsymbol{\sigma}^{i+1}, \kappa^{i+1})}{(\mathbf{a}^{i+1})^{\mathrm{T}}(\mathbf{a}^{i+1})}$$

and the corrected stresses at time t^{i+1} as

$$(\boldsymbol{\sigma}^{i+1})_{\text{corrected}} = \boldsymbol{\sigma}^{i+1} + \beta_1 \mathbf{a}^{i+1}$$

Although computationally expensive, this correction is sometimes applied after each of the substeps ΔT_k.[1]

Although the Euler algorithm with substepping and stress correction has been used widely in finite element programs, it has the following disadvantages:

1. The number of substeps required for each integration point is usually determined by an empirical rule. Since these rules are formulated by trial and error, it is difficult to ensure that the elastoplastic stress–strain relations are integrated with sufficient accuracy for a general type of constitutive law and strain path.
2. There appears to be no theoretical justification for preferring one type of stress correction over another. Indeed a number of different corrections may be formulated which lead to the computed stresses satisfying the yield condition approximately. These corrections, however, do not guarantee that the plastic deformations obey the prescribed flow rule.
3. No estimate of the error in the integration process is available.

The merits of various techniques for integrating elastoplastic stress–strain relations have been discussed by Krieg and Krieg[5] and Schreyer *et al.*[6] Both of these investigations, however, were primarily concerned with the Von Mises yield criterion and did not consider accurate solution algorithms for a general type of constitutive law.

In the numerical analysis literature, efficient methods for solving systems of ordinary differential equations have been derived which attempt to control the errors in the computed solution (see, for example, Reference 7). Broadly speaking these methods may be classified into two categories: single-step and multi-step techniques. Single-step algorithms advance the solution over a step using information generated solely within that step, whereas multi-step algorithms also use information that has been generated in previous steps. In the following sections, two single-step algorithms are described which attempt to control the error in the integration of general constitutive laws. Neither of these methods requires any form of stress correction and each has proved to be a most effective means of integrating the elastoplastic stress–strain relations.

MODIFIED EULER INTEGRATION WITH ERROR CONTROL

For the first-order Euler algorithm, the solution to equations (27) and (28) at the end of a dimensionless time step ΔT_k is given by

$$\boldsymbol{\sigma}_{k+1} = \boldsymbol{\sigma}_k + \Delta\boldsymbol{\sigma}_1 \tag{33}$$

$$\kappa_{k+1} = \kappa_k + \Delta\kappa_1 \tag{34}$$

where

$$\Delta\boldsymbol{\sigma}_1 = \mathbf{D}_{ep}(\boldsymbol{\sigma}_k, \kappa_k)\Delta\boldsymbol{\varepsilon}_k$$

$$\Delta\kappa_1 = \begin{cases} \Delta\lambda(\boldsymbol{\sigma}_k, \kappa_k, \Delta\boldsymbol{\varepsilon}_k)\|\bar{\mathbf{b}}\|_k, & \text{strain hardening} \\ \Delta\lambda(\boldsymbol{\sigma}_k, \kappa_k, \Delta\boldsymbol{\varepsilon}_k)\boldsymbol{\sigma}_k^{\mathrm{T}}\mathbf{b}_k, & \text{work hardening} \end{cases}$$

and $\Delta\boldsymbol{\varepsilon}_k = \Delta T_k \Delta\boldsymbol{\varepsilon}$. The quantities $\|\bar{\mathbf{b}}\|_k$ and $\mathbf{b}_k$ are evaluated at the stress $\boldsymbol{\sigma}_k$. A more accurate estimate of $\boldsymbol{\sigma}_{k+1}$ and κ_{k+1} may be obtained from the modified Euler scheme, which gives

$$\hat{\boldsymbol{\sigma}}_{k+1} = \boldsymbol{\sigma}_k + \tfrac{1}{2}(\Delta\boldsymbol{\sigma}_1 + \Delta\boldsymbol{\sigma}_2) \tag{35}$$

$$\hat{\kappa}_{k+1} = \kappa_k + \tfrac{1}{2}(\Delta\kappa_1 + \Delta\kappa_2) \tag{36}$$

where $\Delta\sigma_1$ and $\Delta\kappa_1$ are given by the Euler scheme, and

$$\Delta\boldsymbol{\sigma}_2 = \mathbf{D}_{ep}(\boldsymbol{\sigma}_{k+1}, \kappa_{k+1})\Delta\boldsymbol{\varepsilon}_k$$

$$\Delta\kappa_2 = \begin{cases} \Delta\lambda(\boldsymbol{\sigma}_{k+1}, \kappa_{k+1}, \Delta\boldsymbol{\varepsilon}_k)\|\bar{\mathbf{b}}\|_{k+1}, & \text{strain hardening} \\ \Delta\lambda(\boldsymbol{\sigma}_{k+1}, \kappa_{k+1}, \Delta\boldsymbol{\varepsilon}_k)\boldsymbol{\sigma}_{k+1}^{\mathrm{T}}\mathbf{b}_{k+1}, & \text{work hardening} \end{cases}$$

and $\|\bar{\mathbf{b}}\|_{k+1}$ and $\mathbf{b}_{k+1}$ are evaluated at the stress $\boldsymbol{\sigma}_{k+1}$.

Now for a given strain increment $\Delta\boldsymbol{\varepsilon}$, the Euler method has a local truncation error of order $O(\Delta T^2)$, whereas the local error in the modified Euler solution is $O(\Delta T^3)$. Thus, subtracting equation (33) from equation (35), we obtain an estimate of the local error in $\boldsymbol{\sigma}_{k+1}$ according to

$$\mathbf{E}_{k+1} \approx \tfrac{1}{2}(-\Delta\boldsymbol{\sigma}_1 + \Delta\boldsymbol{\sigma}_2) \tag{37}$$

This estimate of the local truncation error is only accurate to $O(\Delta T^2)$, but serves as a guide for selecting each substep ΔT_k when integrating from $T = 0$ to $T = 1$. Although the global error in the solution is difficult to monitor directly, it may be controlled by ensuring that the relative error for each substep is less than some specified tolerance. The relative error for a substep is defined as

$$R_{k+1} = \frac{\|\mathbf{E}_{k+1}\|}{\|\boldsymbol{\sigma}_{k+1}\|} \tag{38}$$

and the size of each substep is continually updated during the integration procedure so that

$$R_{k+1} \leqslant \mathrm{TOL} \tag{39}$$

where TOL is a small positive number (typically in the range 10^{-2} to 10^{-5}). A detailed discussion of the theoretical basis for this type of error control may be found, for example, in Reference 7. By controlling the local relative error for each substep, we aim to control the global relative error in the overall solution.

To begin the integration procedure, we first assume a value for ΔT_k and compute $\boldsymbol{\sigma}_{k+1}, \kappa_{k+1}, \hat{\boldsymbol{\sigma}}_{k+1}, \hat{\kappa}_{k+1}, \mathbf{E}_{k+1}$ and R_{k+1} using equations (33)–(38). If equation (39) is satisfied, then the stresses and hardening parameter may be updated using equations (33) and (34) and the integration for this step is complete. If equation (39) is not satisfied then it is necessary to reduce the

size of ΔT_k and repeat the calculation. During the integration procedure the size of each substep is determined by a local extrapolation technique. Step sizes may increase or decrease, depending on the estimated value of R. Assuming that the current substep size is ΔT_k, the next substep size is given by

$$\Delta T_{k+1} = q \Delta T_k \tag{40}$$

where q is positive and greater than zero. Now, since the local error estimate is $O(\Delta T^2)$, we may estimate the local error for ΔT_{k+1} as

$$\|\mathbf{E}_{k+2}\| \approx q^2 \|\mathbf{E}_{k+1}\|$$

In order that equation (39) is satisfied for the next substep we require that

$$\frac{\|\mathbf{E}_{k+2}\|}{\|\boldsymbol{\sigma}_{k+2}\|} \leqslant \text{TOL}$$

Combining the previous two equations and making the approximation that

$$\|\boldsymbol{\sigma}_{k+1}\| \approx \|\boldsymbol{\sigma}_{k+2}\|$$

the required factor q is given by

$$q = \left[\frac{\text{TOL}}{R_{k+1}}\right]^{1/2}$$

Because this procedure is based on local extrapolation, it is usual to choose q conservatively and replace the above equation by

$$q = 0{\cdot}8\left[\frac{\text{TOL}}{R_{k+1}}\right]^{1/2} \tag{41}$$

This helps to reduce the number of substeps that are likely to be rejected during the course of the integration process. In addition, it is wise to introduce limits on the size of each new substep so that the extrapolation is not carried too far. In the current work, ΔT_{k+1} is constrained to lie within the limits

$$0{\cdot}1 \Delta T_k \leqslant \Delta T_{k+1} \leqslant 2 \Delta T_k$$

which implies that

$$0{\cdot}1 \leqslant q \leqslant 2 \tag{42}$$

The overall procedure is started by setting $\boldsymbol{\sigma}_1 = \boldsymbol{\sigma}^i, \kappa_1 = \kappa^i$ and $\Delta T_1 = 1$. During the integration process equations (35) and (36), and not equations (33) and (34), may be used to update the stresses and hardening parameter after a successful step (see, for example, the Runge–Kutta–Fehlberg program in Reference 8). This modification generally leads to an improved solution, since it tends to compensate for the fact that $\mathbf{E}_{k+1}$ is only a truncated estimate of the true local error, and requires that $\boldsymbol{\sigma}_{k+1}$ is replaced by $\hat{\boldsymbol{\sigma}}_{k+1}$ in equation (38).

The modified Euler algorithm, which incorporates error control and a variable step size for each integration point, may now be summarized as follows:

1. Enter with the stresses $\boldsymbol{\sigma}$ and hardening parameter κ, together with the displacement increments for the current load step (or iteration) $\Delta \mathbf{u}$ and the error tolerance TOL.
2. Compute the strains $\Delta \mathbf{e}$ and stress increment $\Delta \boldsymbol{\sigma}$ using equations (19) and (20). If $F(\boldsymbol{\sigma} + \Delta \boldsymbol{\sigma}) \leqslant 0$, set $\boldsymbol{\sigma} \leftarrow \boldsymbol{\sigma} + \Delta \boldsymbol{\sigma}$ and go to step 12.

3. If $F(\boldsymbol{\sigma}, \kappa) < 0$ and $F(\boldsymbol{\sigma} + \Delta\boldsymbol{\sigma}, \kappa) > 0$, compute the portion of $\Delta\boldsymbol{\sigma}$ that causes purely elastic deformation (i.e. compute the α factor as described in the section on initial yielding). If the point underwent plastic yielding in the previous load step or iteration and $F(\boldsymbol{\sigma} + \Delta\boldsymbol{\sigma}, \kappa) > 0$, then set $\alpha = 0$.
4. Compute the portion of $\Delta\boldsymbol{\sigma}$ that causes plastic deformation according to $\Delta\boldsymbol{\sigma}_e = (1 - \alpha)\Delta\boldsymbol{\sigma} = (1 - \alpha)\mathbf{D}\Delta\mathbf{e} = \mathbf{D}\Delta\boldsymbol{\varepsilon}$. Then update the stresses at the onset of plastic yielding according to $\boldsymbol{\sigma} \leftarrow \boldsymbol{\sigma} + \alpha\Delta\boldsymbol{\sigma}_e$.
5. Set $T = 0$ and $\Delta T = 1$.
6. While $T < 1$, do steps 7 to 11.
7. Compute $\Delta\boldsymbol{\sigma}_i$ and $\Delta\kappa_i$ for $i = 1, 2$ according to

$$\Delta\boldsymbol{\sigma}_i = \Delta\boldsymbol{\sigma}_e \Delta T - \Delta\lambda_i \mathbf{D}\mathbf{b}_i$$

$$\Delta\kappa_i = \begin{cases} \Delta\lambda_i \|\bar{\mathbf{b}}\|_i, & \text{strain hardening} \\ \Delta\lambda_i \boldsymbol{\sigma}_i^{\mathrm{T}} \mathbf{b}_i, & \text{work hardening} \end{cases}$$

where

$$\Delta\lambda_i = \max\left\{\frac{\mathbf{a}_i^{\mathrm{T}} \Delta\boldsymbol{\sigma}_e \Delta T}{A_i + \mathbf{a}_i^{\mathrm{T}} \mathbf{D}\mathbf{b}_i}, 0\right\}$$

$$A_i = -\left(\frac{\partial F}{\partial \kappa}\right)\frac{\Delta\kappa_i}{\Delta\lambda_i} \text{ evaluated at } \boldsymbol{\sigma}_i \text{ and } \kappa_i$$

$$\mathbf{a}_i = \frac{\partial F}{\partial \boldsymbol{\sigma}} \text{ evaluated at } \boldsymbol{\sigma}_i$$

$$\mathbf{b}_i = \frac{\partial Q}{\partial \boldsymbol{\sigma}} \text{ evaluated at } \boldsymbol{\sigma}_i$$

and

$$\boldsymbol{\sigma}_1 = \boldsymbol{\sigma}, \quad \kappa_1 = \kappa$$
$$\boldsymbol{\sigma}_2 = \boldsymbol{\sigma} + \Delta\boldsymbol{\sigma}_1, \quad \kappa_2 = \kappa + \Delta\kappa_1$$

8. Compute an estimate of the local truncation error for the substep ΔT according to

$$\mathbf{E} = \tfrac{1}{2}(-\Delta\boldsymbol{\sigma}_1 + \Delta\boldsymbol{\sigma}_2)$$

and compute the new stresses using

$$\hat{\boldsymbol{\sigma}} = \boldsymbol{\sigma} + \tfrac{1}{2}(\Delta\boldsymbol{\sigma}_1 + \Delta\boldsymbol{\sigma}_2)$$

9. Determine the relative error for the substep ΔT from

$$R = \max\left\{\text{EPS}, \frac{\|\mathbf{E}\|}{\|\hat{\boldsymbol{\sigma}}\|}\right\}$$

where EPS is a machine constant indicating the smallest relative error that may be calculated (typically in the range 10^{-14} to 10^{-16} for double precision arithmetic on a 32-bit machine).

10. If $R > \text{TOL}$, then go to step 11. Else, this substep is accepted so update the dimensionless time, the stresses and the hardening parameter according to

$$T \leftarrow T + \Delta T$$

$$\boldsymbol{\sigma} = \hat{\boldsymbol{\sigma}}$$

$$\kappa \leftarrow \kappa + \tfrac{1}{2}(\Delta\kappa_1 + \Delta\kappa_2)$$

Then extrapolate to obtain the size of the next substep using equations (40), (41) and (42), i.e. compute

$$q = \min\{0{\cdot}8(\mathrm{TOL}/R)^{1/2}, 2\}$$

and set

$$\Delta T \leftarrow q\Delta T$$

Before returning to step 6, check that the integration does not proceed beyond $T = 1$ by setting

$$\Delta T \leftarrow \min\{\Delta T, 1 - T\}$$

11. This substep has failed, so extrapolate to obtain a smaller dimensionless time step by using equations (40), (41) and (42). First compute

$$q = \max\{0{\cdot}8(\mathrm{TOL}/R)^{1/2}, 0{\cdot}1\}$$

and then set

$$\Delta T \leftarrow q\Delta T$$

before returning to step 6.

12. Exit with stresses at time t^{i+1} given by $\boldsymbol{\sigma}^{i+1} = \boldsymbol{\sigma}$.

Note that in step 7, the incremental forms of equations (16), (17) and (18) are used to compute the stress increments for the modified Euler scheme. Two evaluations of the $\mathbf{D}_{ep}$ matrix and hardening relation are required for each substep and, following Nayak and Zienkiewicz,[1] small round-off errors are accounted for by ensuring that $\Delta\lambda$ is always non-negative. Typical values for TOL, the parameter which controls the error in the integration process, are in the range 10^{-2} to 10^{-5}. For a single load step or iteration in a finite element analysis, inexact integration of the constitutive law will lead to errors in the computed stresses (assuming that some yield has taken place). These errors are distinct from those introduced by other sources such as the loading programme and the assumed spatial discretization. After a number of load steps or iterations, the errors due to inexact integration of the stress–strain law, which emanate from integration points undergoing plastic yielding, will be propagated throughout the finite element grid. In the current work these errors are measured directly by monitoring the computed stresses $\boldsymbol{\sigma}$ and using the relation

$$\mathrm{Error} = \frac{\left\{\sum_{i=1}^{m} [(\boldsymbol{\sigma}_{\mathrm{ref}} - \boldsymbol{\sigma})^{\mathrm{T}}(\boldsymbol{\sigma}_{\mathrm{ref}} - \boldsymbol{\sigma})]_i\right\}^{1/2}}{\left\{\sum_{i=1}^{m} [(\boldsymbol{\sigma}_{\mathrm{ref}})^{\mathrm{T}}(\boldsymbol{\sigma}_{\mathrm{ref}})]_i\right\}^{1/2}} \tag{43}$$

where the subscript i refers to each integration point, m is the total number of integration points in the mesh and $\boldsymbol{\sigma}_{\mathrm{ref}}$ are the 'reference' stresses. The stresses $\boldsymbol{\sigma}$ and $\boldsymbol{\sigma}_{\mathrm{ref}}$ are computed from finite element analysis with the same mesh, the same sequence of load increments and the same global solution technique; the only difference is that the latter values are determined using a highly accurate scheme for integrating the constitutive law. Note that the stresses $\boldsymbol{\sigma}_{\mathrm{ref}}$ are not exact stresses, since they include errors due to other sources such as the mesh discretization and

the loading programme, but serve as reference stresses to compute the error in the integration process. Analysis of typical boundary value problems, which will be discussed in the applications section of this paper, indicates that the error defined by equation (43) may be controlled directly by adjusting the parameter TOL. Indeed, experience suggests that for many calculations this error measure is approximately equal to TOL.

RUNGE–KUTTA–ENGLAND INTEGRATION SCHEME WITH ERROR CONTROL

In the previous section a modified Euler scheme was described for integrating elastoplastic stress–strain laws. The method was based on first and second-order formulae and varied the size of each substep in an effort to control the error in the integration process. This section describes a similar procedure which is based on a higher order Runge–Kutta scheme.

A set of Runge–Kutta formulae for integrating systems of ordinary differential equations, which employ fourth and fifth order expansions to estimate the local truncation error, has been developed by England.[3] When applied to equations (27) and (28), the fourth and fifth order estimates for the solution after a time step ΔT_k are given, respectively, by

$$\boldsymbol{\sigma}_{k+1} = \boldsymbol{\sigma}_k + \tfrac{1}{6}(\Delta\boldsymbol{\sigma}_1 + 4\Delta\boldsymbol{\sigma}_3 + \Delta\boldsymbol{\sigma}_4) \tag{44}$$

$$\kappa_{k+1} = \kappa_k + \tfrac{1}{6}(\Delta\kappa_1 + 4\Delta\kappa_3 + \Delta\kappa_4) \tag{45}$$

and

$$\hat{\boldsymbol{\sigma}}_{k+1} = \boldsymbol{\sigma}_k + \tfrac{1}{336}(14\Delta\boldsymbol{\sigma}_1 + 35\Delta\boldsymbol{\sigma}_4 + 162\Delta\boldsymbol{\sigma}_5 + 125\Delta\boldsymbol{\sigma}_6) \tag{46}$$

$$\hat{\kappa}_{k+1} = \kappa_k + \tfrac{1}{336}(14\Delta\kappa_1 + 35\Delta\kappa_4 + 162\Delta\kappa_5 + 125\Delta\kappa_6) \tag{47}$$

where

$$\begin{aligned} \Delta\boldsymbol{\sigma}_i &= \mathbf{D}_{ep}(\boldsymbol{\sigma}_i, \kappa)\Delta\boldsymbol{\varepsilon}_k \\ \Delta\kappa_i &= \begin{cases} \Delta\lambda(\boldsymbol{\sigma}_i, \kappa_i, \Delta\boldsymbol{\varepsilon}_k)\|\bar{\mathbf{b}}\|_i, & \text{strain hardening} \\ \Delta\lambda(\boldsymbol{\sigma}_i, \kappa_i, \Delta\boldsymbol{\varepsilon}_k)\boldsymbol{\sigma}_i^{\mathrm{T}}\mathbf{b}_i, & \text{work hardening} \end{cases} \\ \Delta\boldsymbol{\varepsilon}_k &= \Delta T_k \Delta\boldsymbol{\varepsilon} \end{aligned} \tag{48}$$

and

$$\begin{aligned} \boldsymbol{\sigma}_1 &= \boldsymbol{\sigma}_k \\ \boldsymbol{\sigma}_2 &= \boldsymbol{\sigma}_k + \tfrac{1}{2}\Delta\boldsymbol{\sigma}_1 \\ \boldsymbol{\sigma}_3 &= \boldsymbol{\sigma}_k + \tfrac{1}{4}(\Delta\boldsymbol{\sigma}_1 + \Delta\boldsymbol{\sigma}_2) \\ \boldsymbol{\sigma}_4 &= \boldsymbol{\sigma}_k - \Delta\boldsymbol{\sigma}_2 + 2\Delta\boldsymbol{\sigma}_3 \\ \boldsymbol{\sigma}_5 &= \boldsymbol{\sigma}_k + \tfrac{1}{27}(7\Delta\boldsymbol{\sigma}_1 + 10\Delta\boldsymbol{\sigma}_2 + \Delta\boldsymbol{\sigma}_4) \\ \boldsymbol{\sigma}_6 &= \boldsymbol{\sigma}_k + \tfrac{1}{625}(28\Delta\boldsymbol{\sigma}_1 - 125\Delta\boldsymbol{\sigma}_2 + 546\Delta\boldsymbol{\sigma}_3 + 54\Delta\boldsymbol{\sigma}_4 - 378\Delta\boldsymbol{\sigma}_5) \\ \kappa_1 &= \kappa_k \\ \kappa_2 &= \kappa_k + \tfrac{1}{2}\Delta\kappa_1 \\ \kappa_3 &= \kappa_k + \tfrac{1}{4}(\Delta\kappa_1 + \Delta\kappa_2) \\ \kappa_4 &= \kappa_k - \Delta\kappa_2 + 2\Delta\kappa_3 \\ \kappa_5 &= \kappa_k + \tfrac{1}{27}(7\Delta\kappa_1 + 10\Delta\kappa_2 + \Delta\kappa_4) \\ \kappa_6 &= \kappa_k + \tfrac{1}{625}(28\Delta\kappa_1 - 125\Delta\kappa_2 + 546\Delta\kappa_3 + 54\Delta\kappa_4 - 378\Delta\kappa_5) \end{aligned} \tag{49}$$

In equations (48), the quantities $\|\bar{\mathbf{b}}\|_i$ and $\mathbf{b}_i$ are evaluated at the stresses $\boldsymbol{\sigma}_i$, and i ranges from 1 to 6. Subtracting equation (44) from equation (46) we obtain a fifth order estimate of the local truncation error in $\boldsymbol{\sigma}_{k+1}$ according to

$$\mathbf{E}_{k+1} = \tfrac{1}{336}(-42\Delta\boldsymbol{\sigma}_1 - 224\Delta\boldsymbol{\sigma}_3 - 21\Delta\boldsymbol{\sigma}_4 + 162\Delta\boldsymbol{\sigma}_5 + 125\Delta\boldsymbol{\sigma}_6) \tag{50}$$

The theory for devising a Runge–Kutta scheme with variable step size and error control is then identical to that for the modified Euler procedure. For the algorithm described in the previous section, steps 7, 8, 10 and 11 need to be modified as follows:

7. The variable i ranges from 1 to 6 and σ_i and κ_i are given by the equations (49).
8. The estimate of the local truncation error is computed using equation (50). The new stresses are computed using equation (46).
10. The hardening parameter is updated using equation (47) and the factor q is computed from

$$q = \min\{0{\cdot}8(\mathrm{TOL}/R)^{1/5}, 2\}$$

11. The factor q is computed using

$$q = \max\{0{\cdot}8(\mathrm{TOL}/R)^{1/5}, 0{\cdot}1\}$$

For a single substep, the Runge–Kutta–England scheme requires six evaluations of the $\mathbf{D}_{ep}$ matrix and hardening relation. The performance of this algorithm is compared with that of the modified Euler procedure in the next section.

APPLICATIONS

In order to assess the performance of the modified Euler and Runge–Kutta substepping schemes, they have been implemented in a finite element program and applied to a typical boundary value problem. The geometry and mesh for a smooth rigid strip footing resting on an elastoplastic soil mass are shown in Figure 1. This example is selected to test the substepping algorithms since it involves a singularity at the edge of the footing as well as a strong rotation of the principal axes during loading. The element used in all of the analyses is the 15-noded cubic strain triangle. This element is known to give accurate solutions for plasticity problems and does not require the use of a reduced or selective integration rule.[9–12] Under conditions of plane strain the 15-noded triangle requires 12 integration points to evaluate the elastic stiffnesses exactly.

In order to investigate the performance of the proposed procedures, 10 displacement increments of equal size are imposed on the footing. The size of each increment is selected so that the final displacement induces a state of collapse in the soil mass. Two different constitutive laws are used to model the soil layer (one perfectly plastic and the other strain hardening) and the tangent stiffness procedure is employed to solve the governing finite element equations. No iteration is performed during each displacement step, but the unbalanced nodal forces are computed at each stage and applied in the next displacement step (i.e. an Euler procedure with load correction is used). In addition to the load–deformation response, the following quantities are presented for each of the various analyses:

SUMSTP The total number of substeps required for the entire analysis.
MAXSTP The maximum number of substeps required at a single integration point during any displacement increment.
SUMCPU The total CPU time required by the substepping scheme for the entire analysis.

Also, after the 10 displacement increments are applied, the error in the integration of the

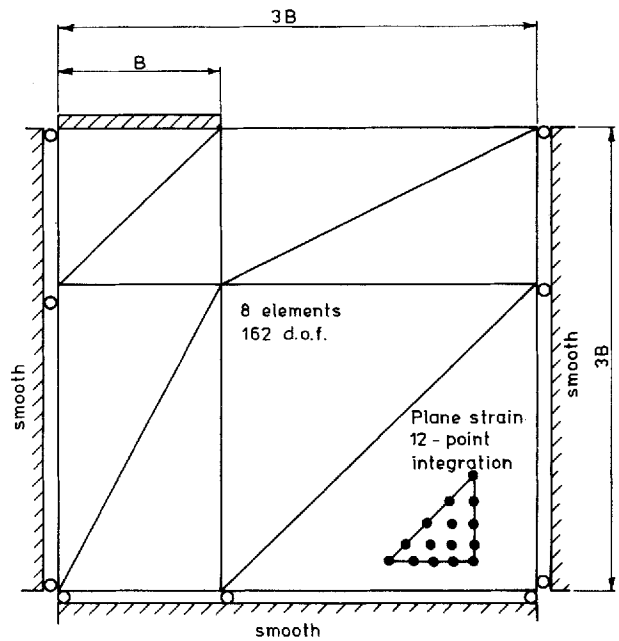

Figure 1. Geometry and mesh for a smooth rigid strip footing on a soil layer

constitutive law is measured using equation (43). The stresses $\boldsymbol{\sigma}_{ref}$ are computed from analysis with the same mesh, the same displacement increments and the same global solution technique, but the Runge–Kutta–England substepping scheme is used to integrate the constitutive law with TOL equal to 10^{-10}. Note that no form of stress correction is used in any of the analyses.

Mohr–Coulomb layer

Figure 2 illustrates various load–deformation curves for a smooth rigid strip footing resting on a Mohr–Coulomb soil mass. The soil is assumed to be perfectly plastic with an associated flow rule, and results are presented for both the modified Euler and Runge–Kutta–England substepping schemes. The singularities in the Mohr–Coulomb yield surface are treated using the method described by Sloan and Booker[13] and the size of each of the 10 displacement increments is 0·005 B, where B is the half-width of the footing. The elastic shear modulus, cohesion friction angle and dilatancy angle of the soil are denoted G, C, ϕ and ψ, respectively. The exact collapse pressure for this problem is 14·83 C.[14] Five results are presented for each of the substepping schemes with values of TOL equal to 1, 10^{-2}, 10^{-3}, 10^{-4} and 10^{-5}. Note that analysis with TOL set equal to 1 does not require any substepping, since the error permitted is quite large.

With reference to Figure 2, both the modified Euler and Runge–Kutta–England procedures give inaccurate load–deformation responses when no substeps are employed. Indeed the former scheme gives no clear indication of impending collapse, whereas the latter scheme yields an oscillatory load–deformation curve. Both algorithms, however, give satisfactory results once TOL is defined to be less than or equal to 10^{-2}. For values of TOL in the range 10^{-2} to 10^{-5}, the modified Euler and Runge–Kutta–England procedures furnish load-deformation curves which are practically identical. These results provide a clear indication of collapse at a pressure which is about 9 per cent above the exact solution.

The statistics associated with the various analyses are shown in Table I. With regard to the

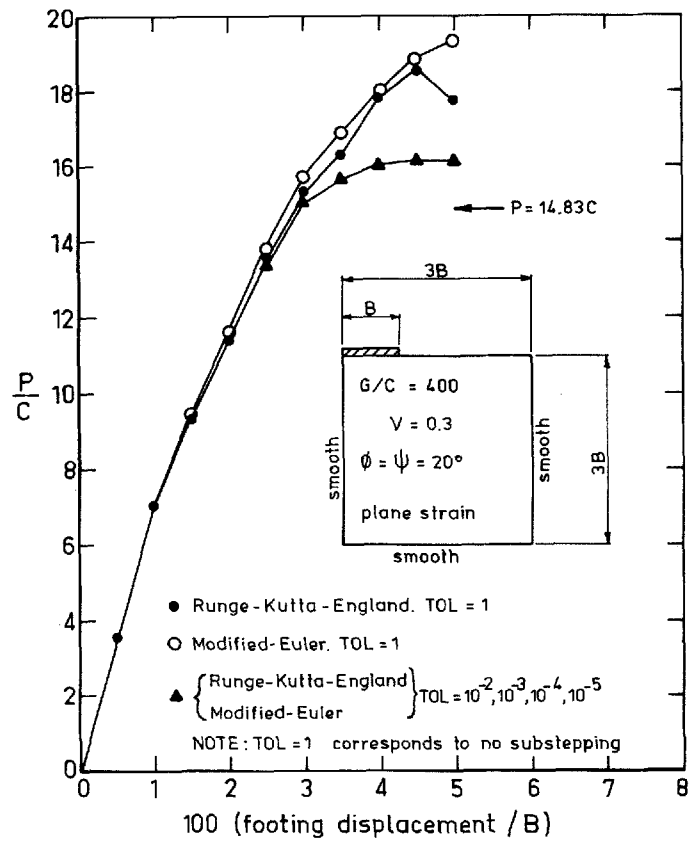

Figure 2. Load–deformation curves for a smooth rigid strip footing on a Mohr–Coulomb layer: effect of error control for modified Euler and Runge–Kutta–England schemes

mechanism for controlling the error in the integration process (as defined by equation (43)), it is apparent that both the modified Euler and the Runge–Kutta–England schemes are particularly effective. After 10 load increments are applied with a value for TOL of 10^{-2}, the modified Euler scheme gives a relative error of $0{\cdot}5 \times 10^{-2}$, whereas the Runge–Kutta–England procedure gives a relative error of $0{\cdot}6 \times 10^{-2}$. For TOL equal to 10^{-5}, the respective errors are $0{\cdot}4 \times 10^{-5}$ and $1{\cdot}5 \times 10^{-5}$. This precision of error control is considered to be adequate for engineering computations. On the topic of efficiency, it is evident that the modified Euler algorithm is superior to the Runge–Kutta–England algorithm for error tolerances in the range 10^{-2} to 10^{-3}. The reverse is true, however, for error tolerances which are smaller than about 10^{-4}, where the relative efficiency of the Runge–Kutta–England scheme increases dramatically. Recalling that the modified Euler and Runge–Kutta–England methods require two and six evaluations, respectively (of the $\mathbf{D}_{ep}$ matrix and hardening relation) per substep, the overall CPU times are in accordance with the numbers of substeps measured.

Strain-hardening Tresca layer

In this section a smooth rigid strip footing, shown in Figure 1, is assumed to rest on an isotropically strain-hardening Tresca layer. An associated flow rule is adopted and the yield

Table I. Statistics for modified Euler and Runge–Kutta–England schemes: smooth rigid strip footing on a Mohr–Coulomb layer

		Error tolerance (TOL)				
		1	10^{-2}	10^{-3}	10^{-4}	10^{-5}
Error	ME	0·2	$0{\cdot}5 \times 10^{-2}$	$0{\cdot}4 \times 10^{-3}$	$0{\cdot}4 \times 10^{-4}$	$0{\cdot}4 \times 10^{-5}$
	RKE	0·2	$0{\cdot}6 \times 10^{-2}$	$0{\cdot}8 \times 10^{-3}$	$1{\cdot}3 \times 10^{-4}$	$1{\cdot}5 \times 10^{-5}$
SUMSTP	ME	498	1384	3105	7514	20,483
	RKE	495	819	1208	1776	2499
MAXSTP	ME	1	13	21	59	178
	RKE	1	12	11	13	16
SUMCPU	ME	2·7	5·8	12·9	27·5	75·8
	RKE	5·9	9·4	14·1	19·8	28·4

Error = error in integration of constitutive law (equation (43)).
SUMSTP = total number of substeps required for the entire analysis.
MAXSTP = maximum number of substeps required at a single integration point during any displacement increment.
SUMCPU = total CPU time required by the substepping scheme for the entire analysis (in seconds for VAX 11/780 operating under VMS).
ME = modified Euler substepping scheme.
RKE = Runge–Kutta–England substepping scheme.

function, written in terms of the principal stresses σ_1 and σ_3, is assumed to be of the form

$$F(\boldsymbol{\sigma}, \kappa) = \tfrac{1}{2}(\sigma_1 - \sigma_3) - C(\kappa) = 0 \tag{51}$$

where $C(\kappa)$, the cohesion of the soil, depends on the history of deformation. Using this yield criterion in conjunction with the isotropic hardening rule described by equations (11), (12) and (13), it may be shown that the hardening parameter is governed by the equation

$$\dot{\kappa} = \dot{\bar{\varepsilon}}_p = \dot{\lambda} \tag{52}$$

The elastoplastic constitutive law is specified completely by assuming that the cohesion varies hyperbolically with κ according to

$$C(\kappa) = C_0 + C_1\left(\frac{\kappa}{\kappa + H}\right) \tag{53}$$

where C_0, C_1 and H are constants. Differentiating equation (51) and using equations (52) and (53), the hardening modulus A is thus

$$A = \frac{HC_1}{(\kappa + H)^2}$$

Figure 3 illustrates various load–deformation curves for a smooth rigid footing resting on the strain-hardening soil mass. Results are presented for both the modified Euler and Runge–Kutta–England substepping schemes and the size of each of the 10 load increments is 0·005 B. For the material properties indicated, the overall cohesion of the yielded soil mass will approach 1·5 C_0 as the plastic strains become large. Thus an upper bound on the exact collapse pressure for the footing is given by the prandtl solution, $(2 + \pi)\, C_0$, times 1·5. As for the Mohr–Coulomb analyses, five

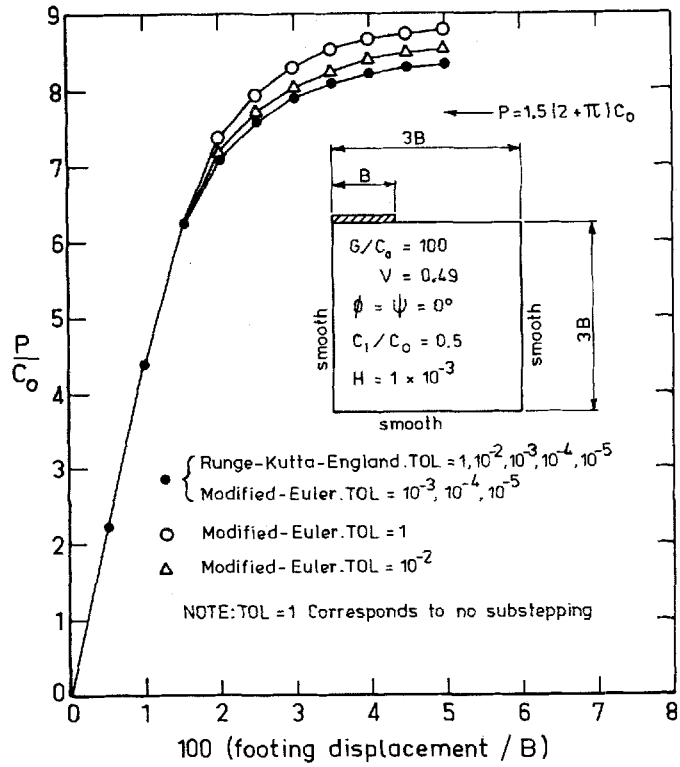

Figure 3. Load–deformation curves for a smooth rigid strip footing on a strain-hardening Tresca layer: effect of error control for modified–Euler and Runge–Kutta–England schemes

results are presented for each of the substepping schemes with values of TOL equal to 1, 10^{-2}, 10^{-3}, 10^{-4} and 10^{-5}.

With reference to Figure 3, it is apparent that the Runge–Kutta–England algorithm is insensitive to the value of TOL for this example. Indeed all of the load–deformation curves for this scheme are practically identical and overestimate the upper bound on the exact collapse load by approximately 8 per cent. In contrast the results for the modified Euler scheme are quite sensitive to the degree of error control. For analysis with no substepping, the load–deformation curve overshoots the upper bound by approximately 14 per cent. Once TOL is set to be smaller than about 10^{-3}, the modified Euler scheme gives results which are practically identical to those for the Runge–Kutta–England scheme.

The statistics for the various strain-hardening analyses are displayed in Table II. The ability of both the substepping schemes to control the error in the integration process, although less good than for the perfectly plastic case, is still satisfactory for engineering purposes. After 10 load increments are applied with a value for TOL of 10^{-2}, the modified Euler and Runge–Kutta–England schemes give relative errors of $2{\cdot}5 \times 10^{-2}$ and $0{\cdot}1 \times 10^{-2}$, respectively. For TOL equal to 10^{-5}, the respective errors are $3{\cdot}3 \times 10^{-5}$ and $1{\cdot}8 \times 10^{-5}$. Examination of these statistics also indicates that the number of substeps for the Runge–Kutta–England algorithm does not increase markedly until TOL is less than about 10^{-3}. This implies that the Runge–Kutta–England scheme, because of its high order, does not need to use substepping to obtain a moderately accurate solution for this problem. With regard to efficiency, the Runge–Kutta–England procedure is superior to the modified Euler algorithm for values of TOL less than about 10^{-3}. Indeed for TOL

Table II. Statistics for modified Euler and Runge–Kutta–England schemes: smooth rigid strip footing on a strain-hardening Tresca layer

		Error tolerances (TOL)				
		1	10^{-2}	10^{-3}	10^{-4}	10^{-5}
Error	ME	$5{\cdot}2 \times 10^{-2}$	$2{\cdot}5 \times 10^{-2}$	$3{\cdot}2 \times 10^{-3}$	$3{\cdot}3 \times 10^{-4}$	$3{\cdot}3 \times 10^{-5}$
	RKE	$0{\cdot}1 \times 10^{-2}$	$0{\cdot}1 \times 10^{-2}$	$0{\cdot}7 \times 10^{-3}$	$1{\cdot}2 \times 10^{-4}$	$1{\cdot}8 \times 10^{-5}$
SUMSTP	ME	626	787	2251	5800	16,404
	RKE	622	622	642	791	1229
MAXSTP	ME	1	6	14	36	109
	RKE	1	1	3	6	8
SUMCPU	ME	3·1	3·5	8·3	21·1	56·2
	RKE	7·0	7·0	7·2	8·9	13·1

Error = error in integration of constitutive law (equation (43)).
SUMSTP = total number of substeps required for the entire analysis.
MAXSTP = maximum number of substeps required at a single integration point during any displacement increment.
SUMCPU = total CPU time required by the substepping scheme for the entire analysis (in seconds for VAX 11/780 operating under VMS).
ME = modified Euler substepping scheme.
RKE = Runge–Kutta–England substepping scheme.

equal to 10^{-5}, the CPU time required by the former scheme is roughly a quarter of the CPU time required by the latter scheme.

CONCLUSIONS

The modified Euler and Runge–Kutta–England algorithms provide a practical means of integrating elastoplastic constitutive laws in finite element analysis. Both procedures control the error in the integration process to within the vicinity of a specified tolerance and assume that the strain increments are known. The mechanism for controlling the integration process permits the size of each substep to vary in accordance with the behaviour of the constitutive law, and is thus efficient. On the basis of the results presented it would appear as though the modified Euler scheme is suitable for error tolerances in the range 10^{-2} to 10^{-3}, whereas the Runge–Kutta–England algorithm is to be preferred for more stringent tolerances. With either method, experience indicates that an error tolerance in the range of 10^{-3} to 10^{-4} is appropriate for most engineering calculations. The procedure outlined is applicable to general constitutive models, including those with non-associated flow.

REFERENCES

1. G. C. Nayak and O. C. Zienkiewicz, 'Elasto-plastic stress analysis: a generalization for various constitutive laws including strain softening', *Int. j. numer. methods eng.*, **5**, 113–135 (1972).
2. D. R. J. Owen and E. Hinton, *Finite Elements in Plasticity: Theory and Practice*, Pineridge Press, West Cross Lane, Swansea, U.K., 1980.
3. R. England, 'Error estimates for Runge–Kutta type solutions to systems of ordinary differential equations', *Computer Journal*, **12**, 166–170 (1969).
4. R. Hill, *The Mathematical Theory of Plasticity*, Oxford University Press, London, 1950.
5. R. D. Krieg and D. B. Krieg, 'Accuracies of numerical solution methods for the elastic perfectly plastic model', *ASME Journal of Pressure Vessel Technology*, **99**, 510–515 (1977).

6. H. L. Schreyer, R. F. Kulak and J. M. Kramer, 'Accurate numerical solutions for elasto-plastic models', *ASME Journal of Pressure Vessel Technology*, **101**, 226–234 (1979).
7. C. W. Gear, *Numerical Initial Value Problems in Ordinary Differential Equations*, Prentice-Hall, New Jersey, 1971.
8. G. E. Forsythe, M. A. Malcolm and C. B. Moler, *Computer Methods for Mathematical Computations*, Prentice-Hall, New Jersey, 1977.
9. S. W. Sloan, 'Numerical analysis of incompressible and plastic solids using finite elements', *Ph. D. Thesis*, University of Cambridge, 1981.
10. S. W. Sloan, 'Plastic collapse calculations using high order elements', *Proceedings of International Conference on Accuracy Estimates and Adaptive Refinements in Finite Element Computations* (*ARFEC*), Lisbon, 19–22 June 1984, pp. 301–313.
11. S. W. Sloan and M. F. Randolph, 'Numerical prediction of collapse loads using finite element methods', *Int. j. numer. anal. methods geomech.*, **6**, 47–76 (1982).
12. R. De Borst and P. A. Vermeer, 'Possibilities and limitations of finite elements for limit analysis', *Geotechnique*, **34**, 199–210 (1984).
13. S. W. Sloan and J. R. Booker, 'Removal of singularities in Tresca and Mohr–Coulomb yield criteria', *Communications in Applied Numerical Methods*, **2**, 173–179 (1986).
14. L. Prandtl, 'Uber die harte plastischer korper', *Gottinger Nachrichten, Math. Phys. Klasse*, 74–85 (1920).